

CHAPTER 4

RESULTS AND DISCUSSION

4.1 EXPERIMENTAL CONDITIONS

In the present study, four parameters that could affect the dispersibility of pigments in polyethylene were investigated. They were the kneading temperature, rotational speed of screw, roller temperature, and median particle size of pigment.

The parameters were varied as follows :

Kneading temperature	:	140, 160, 180, 200 and 220	°C
Rotational speed of screw	:	81, 122, 162, 243, and 324	rpm
Roller temperature	:	57, 67, 77, 87, and 97	°C
Median particle size of pigments:		0.11, 0.17, and 0.20	micrometer

4.2 COMPUTER-SIMULATED RESULTS OF PIGMENT DISPERSIBILITY

Computer-simulated experiments used Monte-Carlo technique to simulate the dispersion of pigment particle in a sample. These computer experiments were used to elucidate the effect of sample population size of pigment particles on the evaluation of pigment dispersibility. Thus the Monte-Carlo approach was used to create random patterns of pigment dispersion. In the present study, two types of random patterns were used, namely, uniform random and normal random

dispersion. A computer code written in the BASIC language (Quick BASIC) was written, which used mathematical functions to generate pseudo uniform random numbers and pseudo normal random numbers to create two different types of dispersion patterns. The objective here was to evaluate pigment dispersibility in terms of the fractal dimension defined by equation (3.3.4) as proposed in the present study and Terashita's fractal dimension and to see how these fractal dimensions were affected by the sample size of pigment population.

4.2.1. Uniform random dispersion

In this case the pigment particles were uniformly but randomly distributed in each resin sample made up of pigment particles and PE resin. The position (X, Y) of a pigment particle on the sample was determined as follows:

$$X = \text{RND} \times \text{XL} \quad (4.1)$$

where

X = the position of pigment particle on the X axis

RND = uniform random number between zero and unity

XL = length of sample piece on the X axis

The position of particle on the Y axis was determined by

$$Y = \text{RND} \times \text{YL} \quad (4.2)$$

With the use of a uniform random number. An example of the uniform random dispersion (sample population size was 64) was shown in Figure 4.1

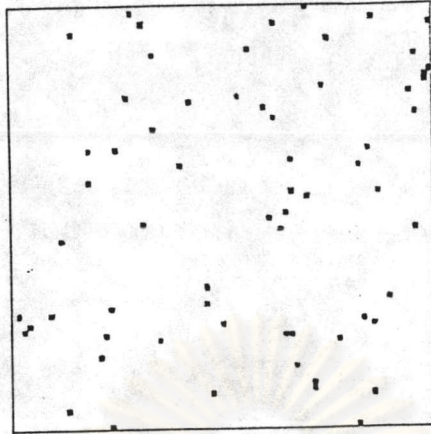


Figure 4.1 Example of the uniform random dispersion of pigment particles obtained from computer simulation

4.2.2. Normal random dispersion

Here the pigment particles were randomly dispersed around the center of a sample according to the normal distribution. The way to determine the position (X, Y) of pigment particle on sample were as follows:

$$X = \text{RNG} \times \sigma_x \quad (4.3)$$

$$Y = \text{RNG} \times \sigma_y \quad (4.4)$$

where

RNG = normal random number (zero mean, unit variance)

X = the position of pigment particle on the X axis

Y = the position of pigment particle on the Y axis

σ_x = standard deviation of variable X

σ_y = standard deviation of variable Y

Of course, different RNG were used for the calculation of each X and each Y. An example of the normal random dispersion (sample population size was 64) is shown in Figure 4.2

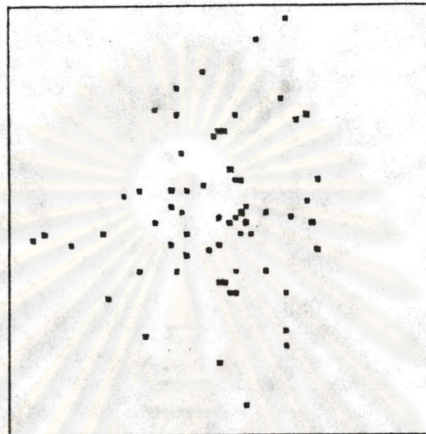


Figure 4.2 Example of the normal random dispersion of pigment particles obtained from the computer simulation

At each similarity ration r , the computer program would count the number of subsections containing at least one pigment particle, $N(r)$, as well as calculate the coefficient of variance (D_s). It was assumed that each pigment particle was uniform in size (equal to one hundredth of the size of the sample) and that each particle existed individually in all the simulations. Then the relationship between $N(r)$ versus r as well as D_s versus r was plotted to determine the fractal dimension for each case of sample population size of pigment particles. Next the relationship between the sample population size and the observed fractal dimension, as defined by equation (3.3.4), was listed in Table 4.1 and plotted in Figure 4.3.

Table 4.1 Computer-simulated results (fractal dimension is found using equation (3.3.4))

Sample population size	Observed fractal dimension (D)	
	uniform random dispersion	normal random dispersion
10	0.0859	0.1837
64	0.4274	0.5345
256	0.9291	0.9800
640	1.279	1.234
1280	1.512	1.408
3200	1.761	1.610
6400	1.890	1.715
12800	1.967	1.801

From Figure 4.3, it can be seen that for both the uniform and normal random dispersion. The observed fractal dimension (D) initially increased rapidly when the sample population size first increased. As the sample population size further increased, the fractal dimension increased more and more gradually. Thus theoretically, the fractal dimension for uniform random dispersion ranged from nearly zero to almost 2, where as the fractal dimension for normal random dispersion ranged from about 0.18 to 1.8. What was most surprising was that the observed fractal dimension for normal random dispersion was greater than that for uniform random dispersion when the sample population size was smaller than 400. Above 400 the observed fractal dimension for uniform random dispersion was, as expected, greater than that for normal random dispersion. At the sample population size around 400, the fractal dimension for both cases was about 1.1. This it means that when the population size was smaller than 400 pigment particles, the normal

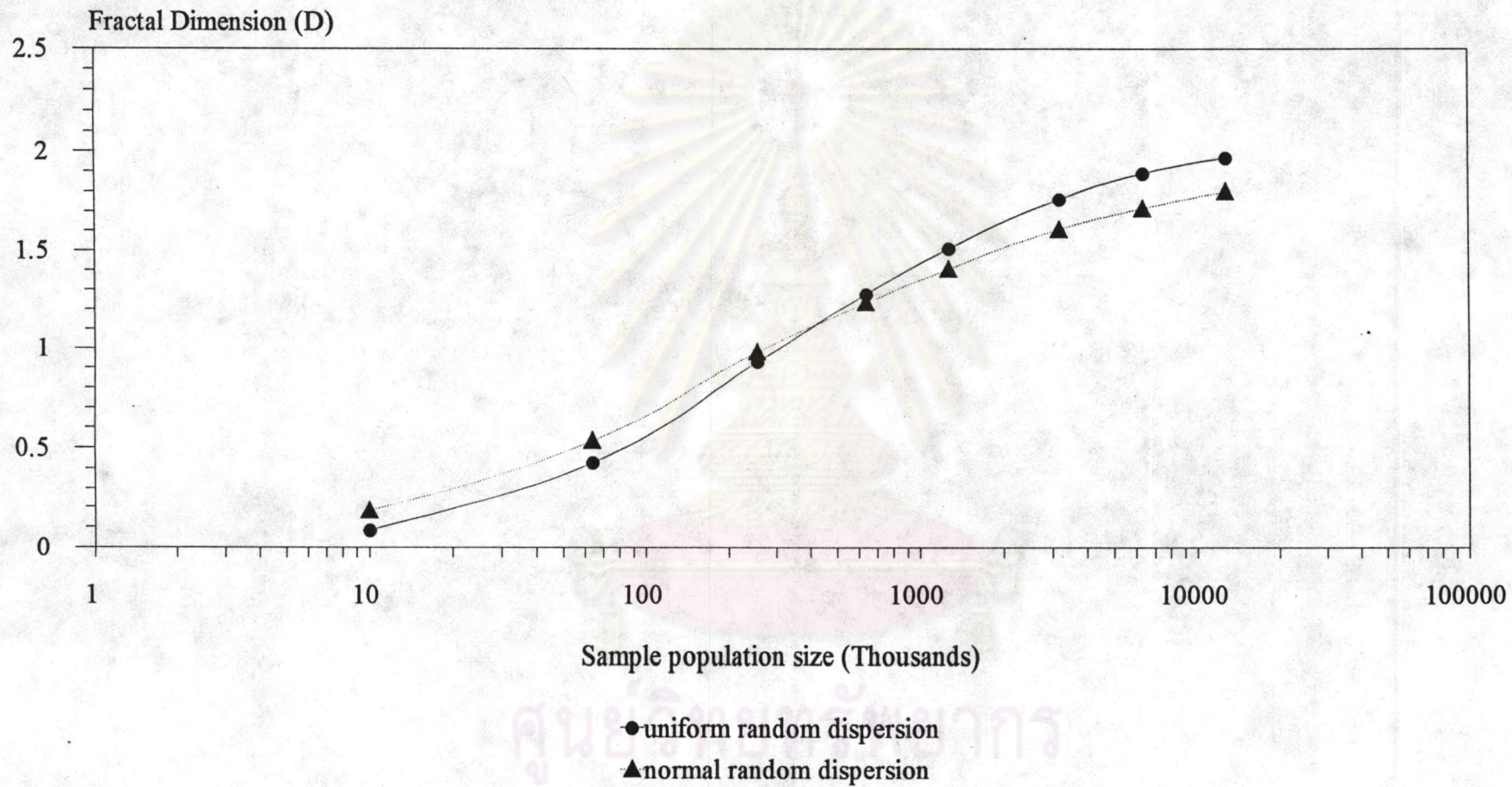
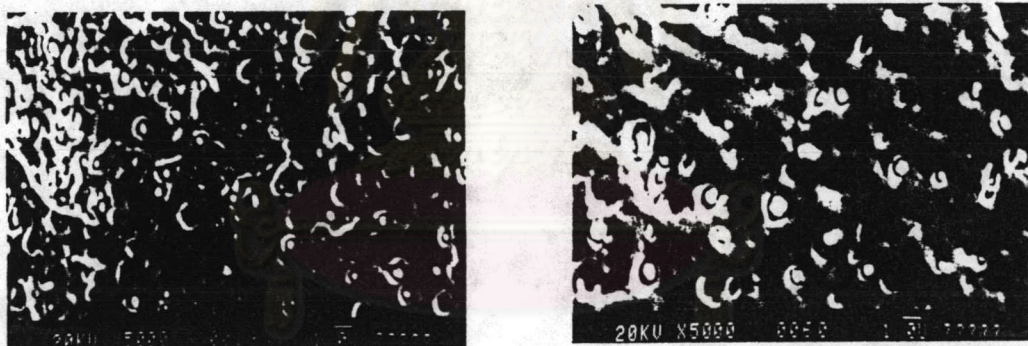


Figure 4.3 Relationship between the observed fractal dimension and the sample population size in the present study

random dispersion, though less uniform, yielded a greater fractal dimension than the uniform random dispersion. The converse was true when the population size was larger than 400. In any case, particle dispersibility should not be evaluated when the sample population size lies between 300 and 500, since the fractal dimensions for both cases show very little difference.

Since the pigment median particle size ($0.1 \sim 0.2 \mu\text{m}$.) in this investigation was very small, a sufficiently high magnifying power was necessary to distinguish between the magnified pigment particles and smudges or even bubbles. It was found that the magnifying power of scanning electron microscope should be 5000X. Figure 4.4 shows two examples of the microphotographs that were taken by SEM in the present study.



$$D = 0.84$$

$$D = 0.96$$

Figure 4.4 Examples of SEM microphotographs

Similarly, the relationship between the sample population size and Terashita's fractal dimension was listed in Table 4.2 and plotted in Figure 4.5.

Table 4.2 Computer-simulated results (Terashita's fractal dimension)

Sample population size	Observed fractal dimension (D)	
	uniform random dispersion	normal random dispersion
10	1.997	1.823
64	2.087	1.413
256	1.990	0.8993
640	2.102	0.6267
1280	2.160	0.4338
3200	2.022	0.2017
6400	1.990	0.0659
12800	1.849	0.0915

From Figure 4.5, it can be seen that the observed Terashita's fractal dimension for uniform random dispersion remained around 2 while the for normal random dispersion dropped rapidly to 0.1 when the sample population size increased.

This means that Terashita's fractal dimension is a more accurate and robust measure of dispersibility than the one defined by equation (3.3.4). In the case of uniform random dispersion, Terashita's fractal dimension remains essentially 2 (between 1.8 to 2.2) regardless of the size of particle population in the test piece. In this case of normal dispersion (non-uniform) Terashita's fractal dimension becomes smaller and smaller as the population size increases.. This confirms the common sense that a certain sufficiently larger sample size is required to differentiate between bad (normal random) and good (uniform random distribution). For Terashita's case, a population size as small as 64 would be enough to clearly differentiate between the two types of dispersion.

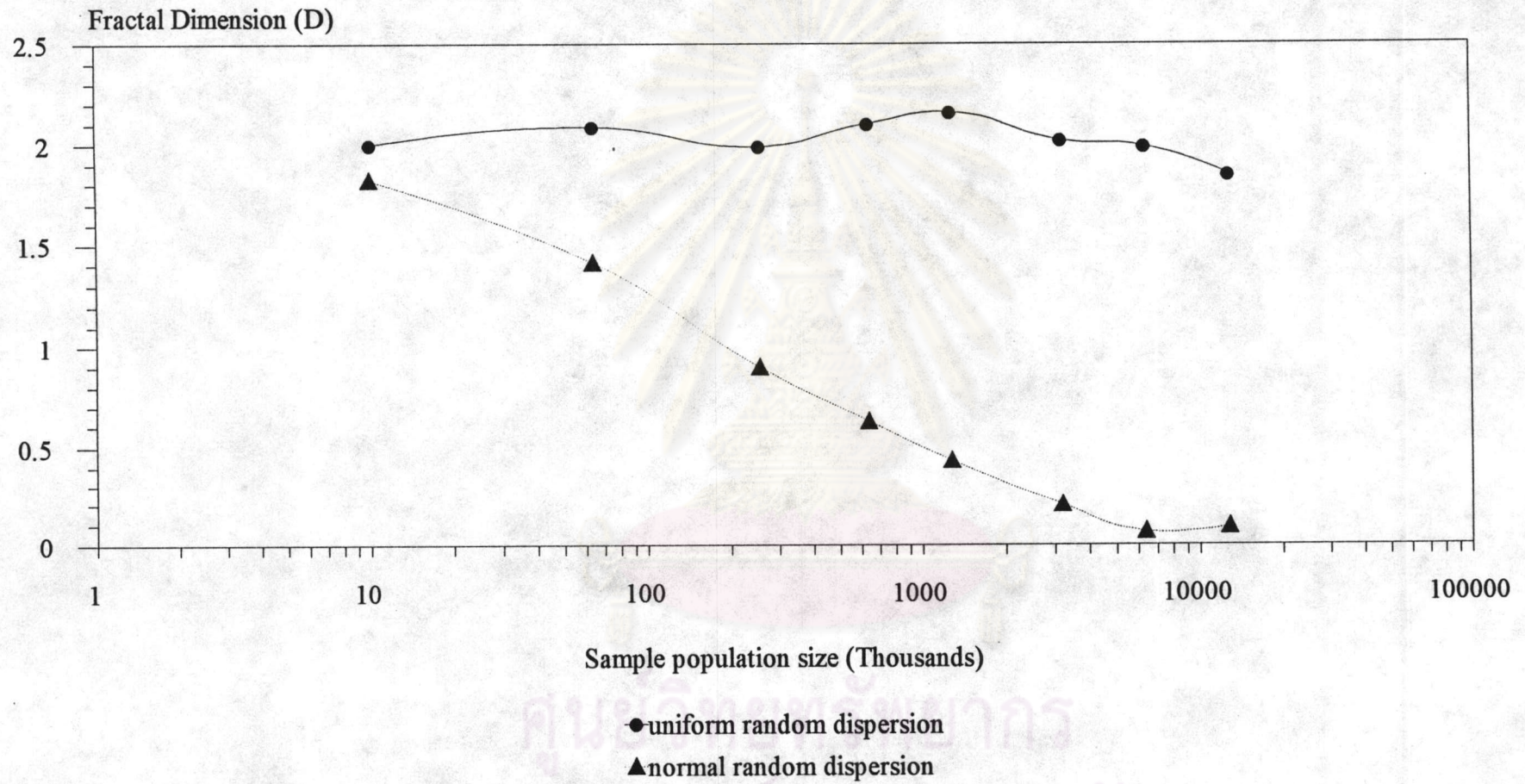


Figure 4.5 Relationship between the observed fractal dimension and the sample population size in Terashita's study

On the other hand, to obtain Terashita's fractal dimension in the present study, it is necessary to use an image analyzer linked to SEM, which was not available. Therefore, the present study cannot but use the fractal dimension defined by equation (3.3.4). Only microphotographs taken by SEM are needed to determine the fractal dimension.

4.3 EFFECTS OF KNEADING CONDITIONS ON THE DISPERSIBILITY OF PIGMENTS IN POLYETHYLENE

In chapter 2, it has been explained that dispersion is achieved through a combination of three mechanisms, i.e. initial wetting, size reduction, and intimate wetting which all occur simultaneously. Initial wetting helps to mix the pigment and carrier together sufficiently well and prevent separation when further work is applied. During mixing of the pigment and plastic, particle-size reduction might occur. Particle-size reduction requires sufficient shear stresses to overcome the structural strength of the particles. If the stresses are smaller than that required to overcome this strength, the particles might not be reduced and dispersed. Intimate wetting facilitates the displacement of air from the pigment surface by carrier. It requires compatibility, like initial wetting, but is more difficult to achieve because much smaller particles are involved. It may be concluded that all of the above mechanisms call for the role of the shear stresses. The shear stresses can be manipulated by the operating temperature, nature of the polymer and speed of mixing.

As mentioned earlier, the present experiments were carried out to study the effects of kneading conditions on the dispersibility of pigments in polyethylene using a continuous kneader. The investigated parameters were the kneading temperature, rotational speed of screw, roller temperature and median particles size of pigment.

The resulting dispersibility of pigment in polyethylene was evaluated using the fractal dimension defined by equation (3.3.4).

4.3.1 Kneading temperature

The effect of the kneading temperature on the dispersibility of the pigment was investigated, at 140, 160, 180, 200 and 220 °C, respectively. The results at these temperatures are summarized in Table 4.3. Figure 4.6 shows the relationship between the observed fractal dimension and kneading temperature.

Table 4.3 Effect of kneading temperature on the dispersibility of pigment in polyethylene (speed of screw 81 rpm, roller temperature 77 °C, and particle size of pigment 0.11 μm .)

No.	Kneading temperature (°C)	Fractal dimension (D)
1	140	0.8186
2	160	0.7436
3	180	0.8589
4	200	0.8667
5	220	0.8577

From Figure 4.6, it can be seen that the fractal dimension initially increased as the kneading temperature first increased. Above 180 °C, the fractal dimension was essentially constant. It showed that the dispersibility of pigment increased as the kneading temperature increased and higher temperature did not affect the dispersion of the pigment. However, at 200°C, the pigment will disperse better in polyethylene than at any other kneading temperatures.

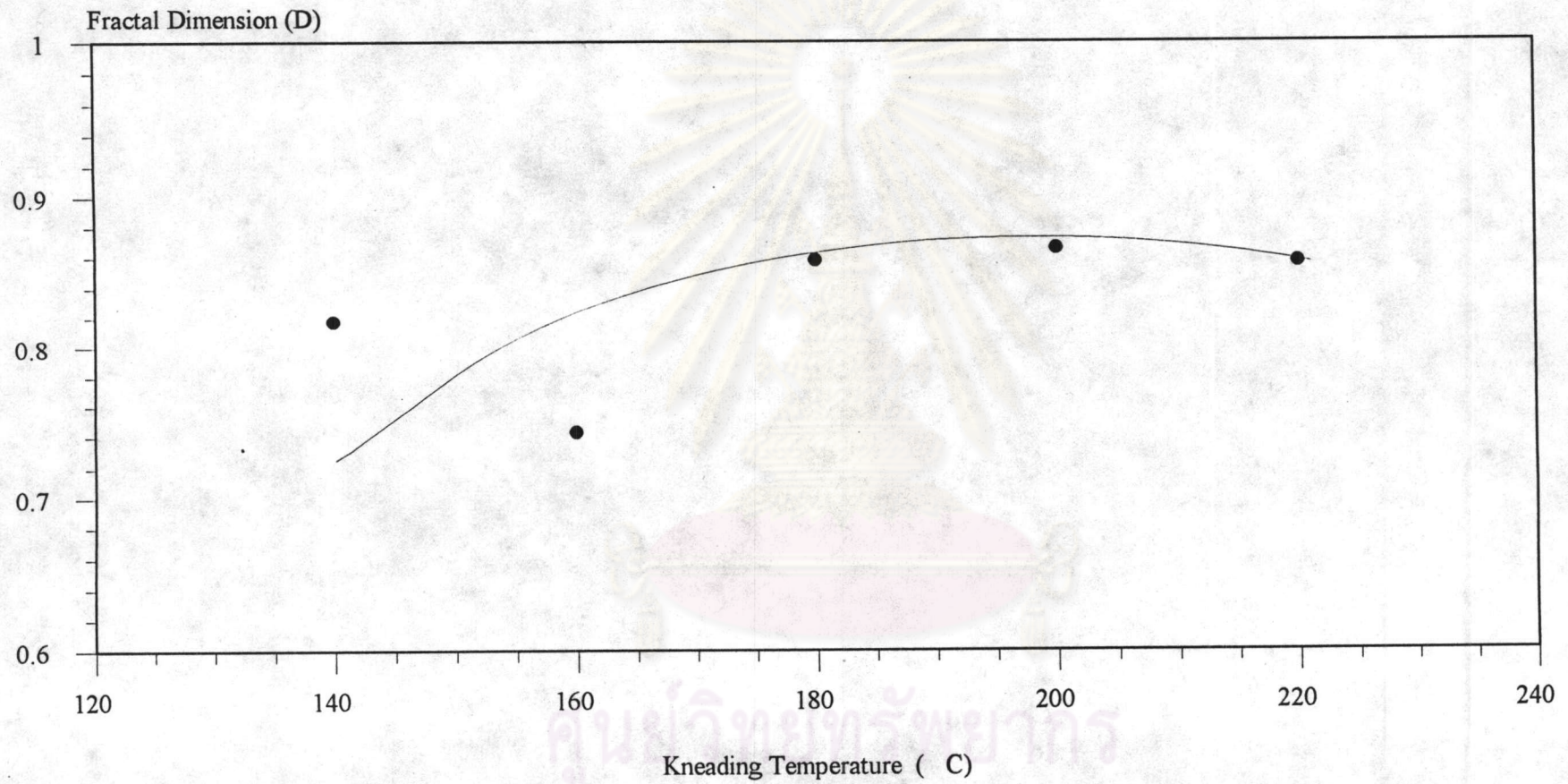


Figure 4.6 Relationship between the kneading temperature and the fractal dimension

4.3.2 Rotational speed of screw

Here the effect of the rotational speed of the twin screws on the dispersibility of the pigment was investigated at 81, 122, 162, 243, and 324 rpm., respectively. The observed fractal dimension is listed in Table 4.4. and shown graphically in Figure 4.7.

Table 4.4 Effect of the rotational speed of screw on the dispersibility of pigment in polyethylene (kneading temperature 140°C, roller temperature 77°C, and particle size of pigment 0.11 μm .)

No.	Speed of screw (rpm)	Fractal dimension (D)
1	81	0.8186
2	122	0.8784
3	162	0.9344
4	243	0.8401
5	324	0.9601

From Figure 4.7, it can be seen that the observed fractal dimension increased as the rotational speed of the twin screws of this continuous kneader increased. At 243 rpm., the observed fractal dimension was lower than both at 162 rpm. and 324 rpm. though the kneading energy was proportional to the square of the speed of screw. However, the overall trend shows that the observed fractal increased as the rotational speed of screw increased. Therefore at 324 rpm., the pigment dispersed best in polyethylene.

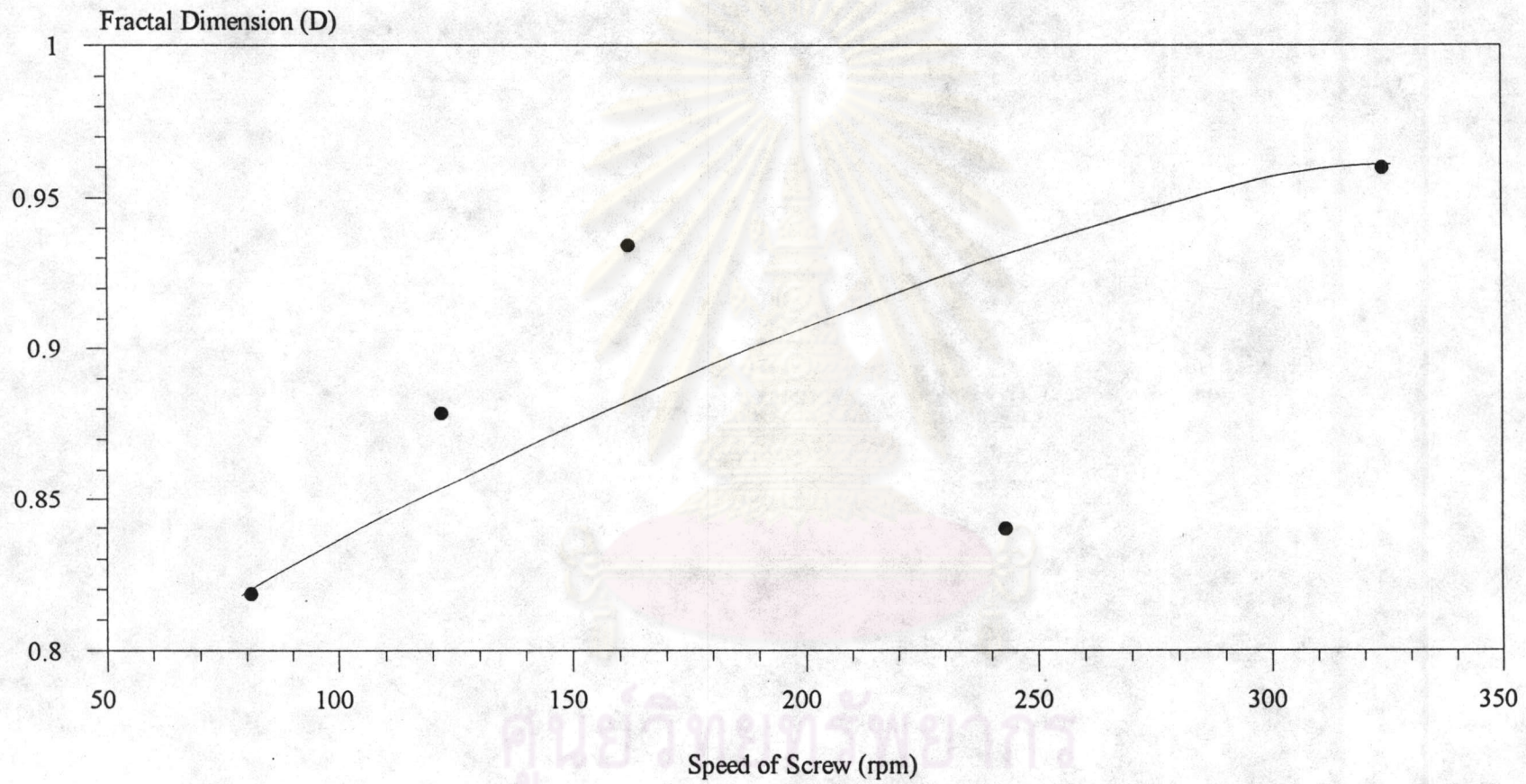


Figure 4.7 Relationship between the rotational speed of screw and the fractal dimension

4.3.3 Roller temperature

The effect of the roller temperature on the dispersibility of pigment was investigated at 57, 67, 77, 87 and 97 °C, respectively. The resulting fractal dimension is listed in Table 4.5., and shown in Figure 4.8.

Table 4.5 Effect of roller temperature on the dispersibility of pigment in polyethylene (kneading temperature 180 °C, speed of screw 81 rpm., and particle size of pigment 0.11 μm .)

No.	Mold temperature (°C)	Fractal dimension (D)
1	57	0.8921
2	67	0.8109
3	77	0.8589
4	87	0.8747
5	97	0.8608

From Figure 4.8, it can be seen that the fractal dimension was essentially independent of the roller temperature. This means that the roller temperature did not significantly affect the dispersibility of the pigment in polyethylene.

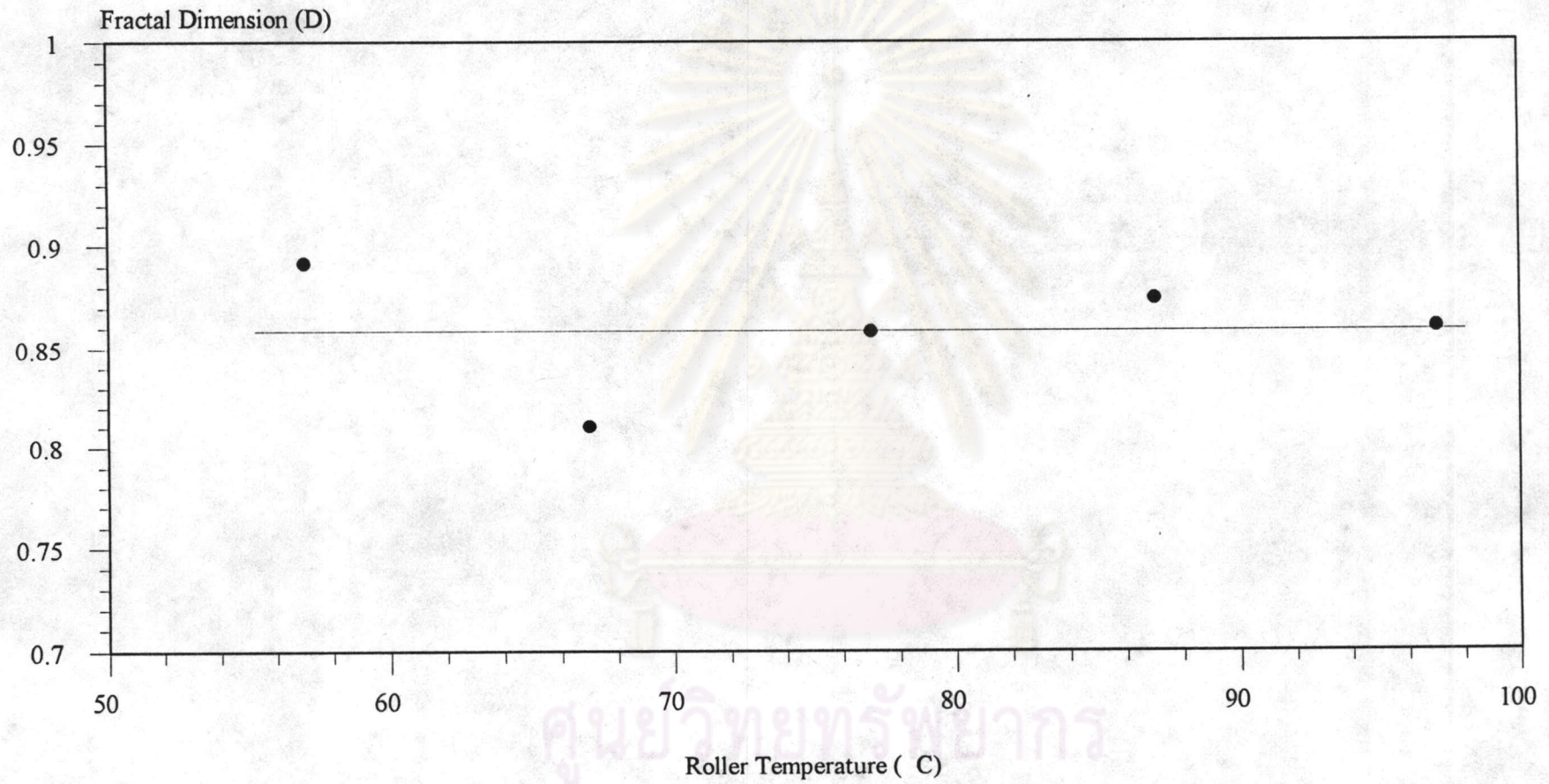


Figure 4.8 Relationship between the roller temperature and the fractal dimension

4.3.4 Particle size of pigment

The effect of particle size of pigment on the dispersibility of pigment was investigated at 0.11, 0.17, and 0.20 μm . median size, respectively. The results are listed in Table 4.6. and shown in Figure 4.9.

Table 4.6 Effect of particle size of pigment on the dispersibility of pigment in polyethylene (kneading temperature 140 °C, speed of screw 81 rpm., and roller temperature 77 °C)

No.	Particle size of pigment (μm)	Fractal dimension (D)
1	0.11	0.8186
2	0.17	0.9657
3	0.20	0.9673

Since only three particle sizes were tested, it can not be concluded with high certainty which particle size gave the best dispersibility. Nevertheless, from Figure 4.9, it can be seen that the fractal dimension increased as the particle size of pigment increased. Thus, of the three particle sizes of pigment, the 0.20 μm . gave the best dispersion in polyethylene.

From the above experimental results, it may be concluded that the most suitable kneading temperatures was 200 °C. Above this temperature the process became more of mixing than dispersion because of the greater fluidity. Regarding the rotational speed of the twin screws, a higher rotational speed yielded higher dispersion because it raised the intensity of energy input and led to an increased level of shear stresses passed through the kneaded material. The highest rotational speed of 324 rpm. was the most suitable.

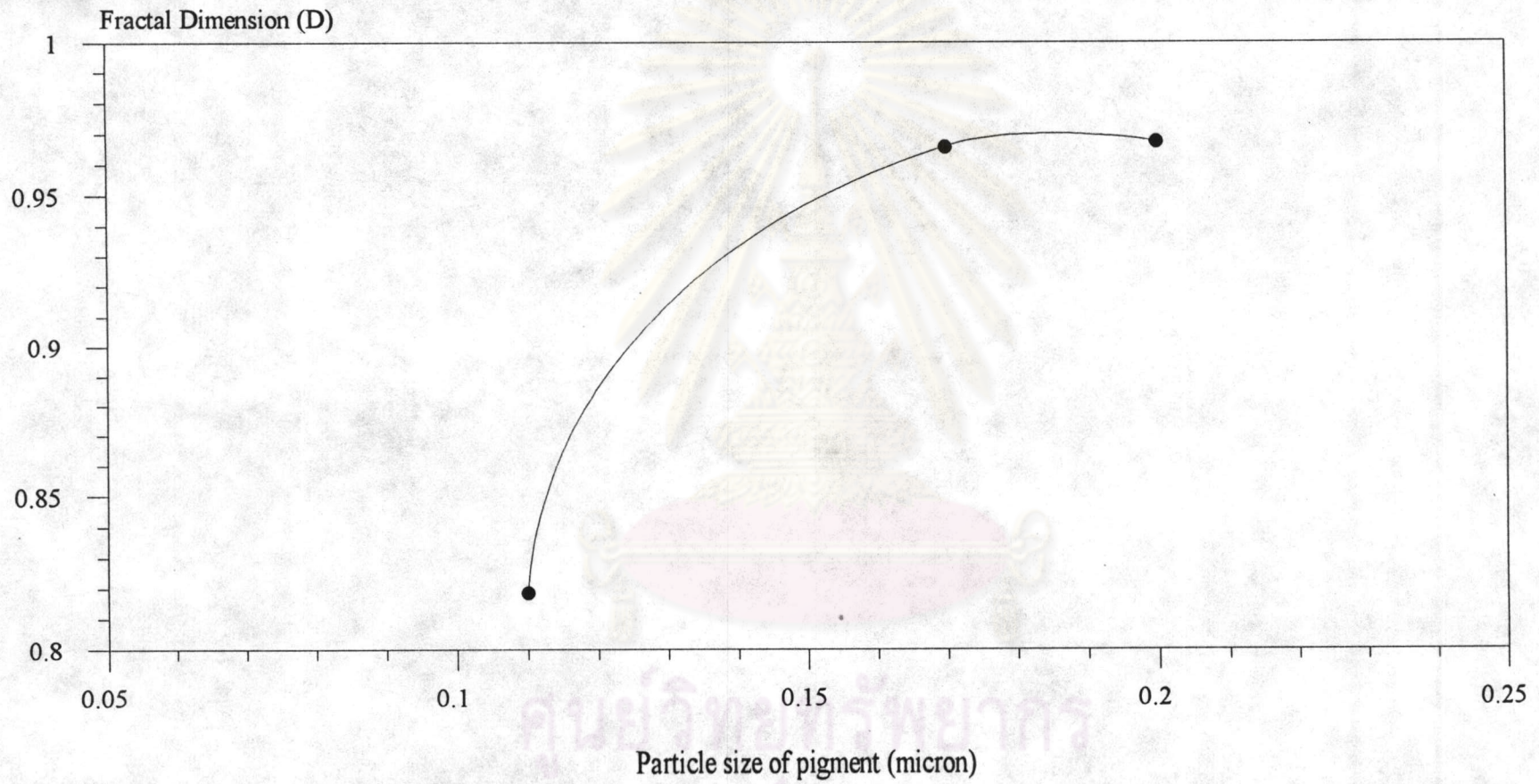



Figure 4.9 Relationship between the particle size of pigment and the fractal dimension

The press rollers were used to spread the melt coming out of the kneader into thin sheets. During pressing, pigment particles would be spread out, which affected only the internal structure between pigment and polyethylene. Thus the roller temperature should not affect the dispersibility of pigment in polyethylene. As mentioned in chapter 2, dispersibility could vary significantly with agglomerate size. Our results show that the suitable particle size of pigment, from among the three particle sizes studied, was 0.20 μm .



ศูนย์วิทยทรัพยากร
จุฬาลงกรณ์มหาวิทยาลัย

4.4 COMPARISON OF EXPERIMENTAL AND COMPUTER-SIMULATED RESULTS

The fractal dimensions obtained experimentally and by computer simulation are compared here. A summary of the experimental results was shown in Table 4.7.

Table 4.7 The experimental results

Particle size of pigment (μm .)	Kneading temperature ($^{\circ}\text{C}$)	Mold temperature ($^{\circ}\text{C}$)	Rotational speed of screw (rpm.)	Fractal dimension
0.11	140	77	81	0.8186
0.11	160	77	81	0.7436
0.11	180	77	81	0.8589
0.11	200	77	81	0.8667
0.11	220	77	81	0.8577
0.11	180	57	81	0.8921
0.11	180	67	81	0.8109
0.11	180	77	81	0.8589
0.11	180	87	81	0.8747
0.11	180	97	81	0.8608
0.11	140	77	81	0.8186
0.11	140	77	122	0.8784
0.11	140	77	162	0.9344
0.11	140	77	243	0.8401
0.11	140	77	324	0.9601
0.11	140	77	81	0.8186
0.17	140	77	81	0.9657
0.20	140	77	81	0.9673

To compare the results of Table 4.7 with computer-simulated ones, it is necessary to estimate the number of particles that were present in the sample. It was estimated that there were on average 239, 65, and 40 particles present for pigment size of 0.11, 0.17, and 0.20 μm ., respectively. Table 4.8 shows the corresponding computer-simulated results that have been obtained under the assumptions of no size reduction and no aggregation or agglomeration.

Table 4.8 The computer-simulated results (no size reduction, no aggregation)

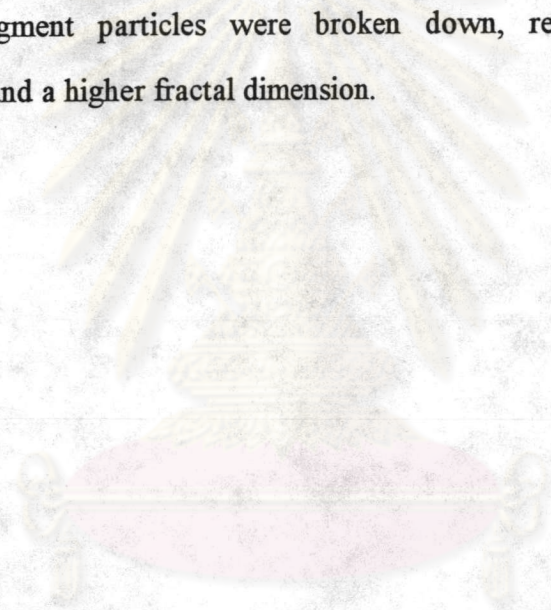
Particle size of pigment (μm .)	Amount of particle in sample (particle)	Fractal dimension (D)	
		uniform random dispersion	normal random dispersion
0.11	239	0.90	0.95
0.17	65	0.40	0.55
0.20	40	0.30	0.40

The comparison of experimental and computer-simulated results is shown in Table 4.9.

Table 4.9 Comparison of experimental and computer-simulated results

Particle size of pigment (μm .)	Estimated sample size (particle)	Fractal dimension (D)		
		Computer simulation		Experiments
		uniform random dispersion	normal random dispersion	
0.11	239	0.90	0.95	0.8196
0.17	65	0.40	0.55	0.9657
0.20	40	0.30	0.40	0.9673

In studying the effects of kneading temperature, the rotational speed of screw, and the roller temperature, the median particle size of the pigment used was 0.11 μm . When compared with the corresponding computer-simulated results, most of the observed fractal dimensions of the experimental results in Table 4.7 were slightly less than the computer-simulated results. It indicates that the actual pigment particles agglomerate together, resulting in a larger size and smaller fractal dimension. For pigment particle size of 0.17 and 0.20 μm ., the experimental fractal dimension were significantly higher than the computer-simulated results. It indicates that pigment particles were broken down, resulting in a smaller agglomerate size and a higher fractal dimension.



ศูนย์วิทยทรัพยากร
จุฬาลงกรณ์มหาวิทยาลัย

4.5 EFFECT OF KNEADING ENERGY ON PIGMENT DISPERSIBILITY

Naruo Yabe, Keijiro Terashita, Kiichi Izumida, and Kei Miyanami (1988) studied the dispersion of carbon black in resin when a similar continuous kneader was applied. Their dispersion results were, however, evaluated by using ASTM-D-2663-69 (See chapter 3).

Figure 4.10 shows the relationship between the degree of dispersion and the kneading energy (Yabe, 1988)

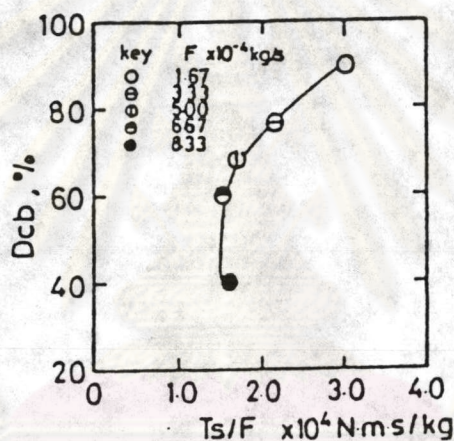


Figure 4.10 Relationship between the degree of dispersion and the kneading energy

From Figure 4.10, it can be seen that the degree of dispersion increased as the kneading energy increased. This is in agreement with the effect of the speed of the screw in the present study. When the speed of screw increased, the kneading energy would increase in proportion and when the kneading energy increased, the particle dispersibility would also increase.